PARTITIONED FINITE ELEMENT ANALYSIS OF SHELL STRUCTURES UNDER BLAST WAVES

Allan Y. Suzuki

Rodolfo A. K. Sanches

allan.suzuki@usp.br

rodolfo.sanches@usp.br

Escola de Engenharia de São Carlos, Universidade de São Paulo

Avenida Trabalhador são-carlense, 400, Pq Arnold Schimidt. Zip-Code 13566-590, São Carlos, SP, Brazil

Abstract. *In this work we study fluid-structure coupling of short duration events, such as blast waves. During such problems, a large amount of energy is liberated in a very localized way, producing a region of high pressure expanding supersonically, followed by a subsonic flow. In order to have a good comprehension of such effects, it is necessary to carry an analysis not only considering the estimated impact forces over the structure, but also the coupling between fluid flow and the deformable structure. In this work we explore how to couple a compressible fluid dynamics solver to a nonlinear shell dynamics solver in order to precisely model these problems. One-way and two-way partitioned coupling techniques are considered and different time steps are allowed to fluid and structure. The fluid flow is modeled by linear tetrahedral finite elements using an explicit time integrator using arbitrary Lagrangian Eulerian description, while the structure is modeled by shell elements using a energy functional Lagrangian formulation with positions as nodal parameters instead of displacement, allowing to employ the implicit Newmark time integrator for large displacement problems. A couple numerical examples are used to analyse the effect of time step and different coupling algorithm and results.*

Keywords: *Fluid Structure Interaction, Finite Element Method, ALE, CFD, Computational Solid Dynamics.*

1 INTRODUCTION

Many structures can be subject to blast waves during its life period, accidentally (specially in industrial plants) or due to war actions. Aiming to avoid major damages, it is important to consider such effects during project. Experimental analysis are reliable, but very expensive and applicable to the tested situation and geometry. This makes the numerical analysis the best alternative, which is widely investigated by several authors, since mathematical models for such problems are extremely complex and, in general, do not have an analytical solution.

Fluid structure interaction problems involving blast waves, such as explosions, are not simple due to the presence of strong discontinuities (major details are given by:Taylor et al. (1998); Bethe et al. (1947); Prümmer (2009)) and the employment of unsuitable numerical methods, leads to undesirable numeric solutions, called spurious oscillations. Thus, an efficient tool should be able to model the pressure peaks, in robust and credible way.

In order to make a precise analysis of the behavior of elastic bodies subjected to the blast wave, it is necessary to perform a fluid-structure interaction analysis (FSI). FSI numerical modeling necessarily consists in three main problems: computational fluid mechanics, computational solid mechanics and interaction problem (Sanches and Coda, 2013).

In this paper we study how to couple a shell dynamics fem solver to a compressible flow fem solver in an efficient way to solve the problems described above.

The compressible flow governing equations are very suitable for explicit algorithms based on systems that can be solved at each time step by mass matrix inversion. This allows us to lump the mass matrix and save considerable computing time, as the fluid domain in general is much larger than the structure domain. On the other hand, the number of degrees of freedom for shell structures is much smaller, and at same time, exact deformation kinematics is desired, giving momentum for the choice of implicit time integration.

In order to take in account the allow moving boundaries, the fluid governing equations are written in the Arbitrary Lagrangian-Eulerian Description (ALE), allowing the fluid domain to be deformed following the Lagrangian shell displacements.

The structure is modeled by shell finite elements, as it makes possible to simulate the majority of two- or three-dimensional structural problems at low cost compared to solid elements. The numerical dynamic shell solver is based on the positional finite element formulation, introduced by Bonet et al. (2000) and Coda (2003) in the frame finite element context, and described in details for large displacement shell dynamics by Sanches and Coda (2013). The main advantages of the positional shell formulation is that it has no rotation degrees of freedom, avoiding the need for large rotation approximations, presenting constant mass matrix, and allowing the use of Newmark time integrator in a stable way (Sanches and Coda, 2013).

The interaction problem can be solved in monolithic way, in which the fluid and solid domain are treated as a unique domain along time, or in partitioned way, where fluid and the solid are integrated in time separately and interface conditions are exchanged from one code to the other. Many different strategies are possible for a partitioned coupling scheme. Among all the partitioned schemes, two of them stand out: one-way coupling, in which occurs only the fluid flow forces are transmitted to the structure, while the fluid domain remains insensible to solid displacements and velocities; and two-way coupling, in which both fluid and solid effects are transmitted from one to the other. In this work we study the effect of one-way and two-

way partitioned coupling, allowing different time-steps for fluid and structure, for analysis of structures under shock waves.

2 COMPRESSIBLE FLUID NUMERICAL ANALYSIS

2.1 ALE formulation

The ALE description of the continuum movement is obtained by introducing a reference domain with arbitrary movement, Fig. 1, where R, $C(t_0)$ and $C(t)$ are, respectively, the reference domain, initial and final configuration based on the moving reference domain (Sanches, 2011).

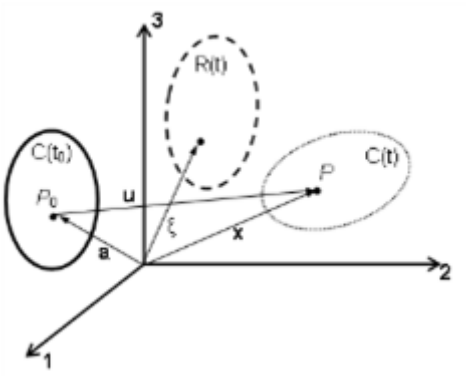

Figure 1: Adopted kinematics for ALE description.

The Jacobian J, for the transformation from the reference domain $R(t)$ to the material domain $C(t_0)$, is given by:

$$J = det(A), \text{ where } A_{ij} = \frac{\partial \xi_i}{\partial a_j} \text{ with } i \text{ and } j = 1, 2 \text{ or } 3 \ , \tag{1}$$

where ξ_i and a_j are the position vectors components regarding respectively to $R(t)$ and $C(t_0)$.

Considering a physical property expressed on the reference configuration as $f(\xi_i, t)$ and equal to $F(a_i, t)$ on the initial configuration, and the velocity vector of the reference domain $\nabla(f\mathbf{w})$, it can be deduced (see Donea et al. (1982)):

$$\frac{\partial (JF)}{\partial t} = J\left[\frac{\partial f}{\partial t} + \nabla \cdot (f\mathbf{w})\right]. \tag{2}$$

Substituting $f = \rho$ (density) in Eq. (2) and considering the mass conservation equation in the Eulerian description ($\partial\rho/\partial t + \partial(\rho u_i)/\partial x_i = 0$), adopting index notation we have:

$$\frac{\partial \rho}{\partial t} + \frac{\partial (\rho u_i)}{\partial t} = w_i \frac{\partial \rho}{\partial x_i}, \tag{3}$$

which is the mass conservation equation in ALE description. Similarly, following the same procedures for momentum and for energy, we have respectively:

$$\frac{\partial(\rho u_i)}{\partial t} = -\frac{\partial(u_j \rho u_i)}{\partial x_j} + w_j \frac{\partial(\rho u_i)}{\partial x_j} + \frac{\partial \tau_{ij}}{\partial x_j} - \frac{\partial p}{\partial x_i} + \rho g_i, \tag{4}$$

$$\frac{\partial(\rho E)}{\partial t} = -\frac{\partial(u_j \rho E)}{\partial x_j} + w_j \frac{\partial(\rho E)}{\partial x_j} + \frac{\partial}{\partial x_i}\left(k \frac{\partial T}{\partial x_i}\right) - \frac{\partial(u_j p)}{\partial x_j} + \frac{\partial(\tau_{ij} u_j)}{\partial x_j} + \rho g_i u_i. \tag{5}$$

It is important to observe that if the velocity w is null, the formulation relies on the Eulerian description, while, if $w = u$, relies on the Lagrangian description.

2.2 Time discretization

We adopt an explicit algorithm proposed by Zienkiewicz and Roriva (1993), in pure explicit version (Sanches and Coda, 2014), in three steps. Integrate respectively equations (4),(3) and (5), we have the three steps summarized as:

1. Calculate the momentum variation

$$\begin{aligned}\Delta(\rho u_i)_{n+1} = \Delta t \left(-\frac{\partial(u_j \rho u_i)}{\partial x_j} + w_j \frac{\partial(\rho u_i)}{\partial x_j} + \frac{\partial \tau_{ij}}{\partial x_j} - \frac{\partial p}{\partial x_i} + \rho g_i\right)_n + \\ \frac{\Delta t^2}{2}\left(u_k \frac{\partial}{\partial x_k}\left(\frac{\partial(u_j \rho u_i)}{\partial x_j} - w_j \frac{\partial(\rho u_i)}{\partial x_j} - \frac{\partial \tau_{ij}}{\partial x_j} + \frac{\partial p}{\partial x_i} - \rho g_i,\right)\right)_n,\end{aligned} \tag{6}$$

2. Calculate the density variation

$$\Delta\rho_{n+1} = -\Delta t \left(\frac{\partial(\rho u_i)_n}{x_i} + \theta \frac{\partial(\Delta(\rho u_i))_{n+1}}{\partial x_i} + w_i \frac{\partial \rho}{\partial x_i}\right)_n + \frac{\Delta t^2}{2} u_k \frac{\partial}{\partial x_k}\left(-w_i \frac{\partial \rho}{\partial x_i}\right)_n, \tag{7}$$

3. Calculate the energy variation and the secondary variable to the next step

$$\begin{aligned}\Delta(\rho E)_{n+1} = \Delta t \left(-\frac{\partial(u_i \rho E)}{\partial x_i} + w_i \frac{\partial(\rho E)}{\partial x_i} + \frac{\partial}{\partial x_i}\left(k \frac{\partial T}{\partial x_i}\right)\right) + \\ \Delta t \left(-\frac{\partial(u_i p)}{\partial x_i} + \frac{\partial(\tau_{ij} u_j)}{\partial x_i} - \rho g_i u_i\right)_n + \\ \frac{\Delta t^2}{2} u_k \frac{\partial}{\partial x_k}\left(\frac{\partial(u_i \rho E)}{\partial x_i} - w_i \frac{\partial(\rho E)}{\partial x_i} - \frac{\partial}{\partial x_i}\left(k \frac{\partial T}{\partial x_i}\right)\right) + \\ \frac{\Delta t^2}{2} u_k \frac{\partial}{\partial x_k}\left(\frac{\partial(u_i p)}{\partial x_i} - \frac{\partial(\tau_{ij} u_j)}{\partial x_i} + \rho g_i u_i\right)_n,\end{aligned} \tag{8}$$

The constant θ in (7) is an arbitrary with value between 0.5 and 1.0.

Applying the Bubnov-Galerkin method to Eq. (6), (8) and (7), we obtain the spatial discretization and solve the resulting system getting the week solution. We still need to deal with the discontinuities due to the presence of shock waves, as the standard Galerkin method is unable to deal with strong discontinuities. Therefore, the artificial diffusion term based on pressure second derivative is added:

$$f_{\mu_a} = \Delta t \mu_a \frac{\partial}{\partial x_i}\left(\frac{\partial \phi}{\partial x_i}\right), \tag{9}$$

where ϕ is the variable to be smoothed and μ_a is the artificial viscosity given by:

$$\mu_a = q_{dif} h^3 \frac{|u| + c}{p_{av}} \left| \frac{\partial}{\partial x_i}\left(\frac{\partial p}{\partial x_i}\right)\right|_e, \tag{10}$$

where $|u|$ is the velocity absolute value, p_{av} is the pressure average over the element, q_{dif} is an user specified coefficient taken between 0 and 2, c is the sound speed and h is the element size (Zienkiewicz and Taylor, 2000; Nithiarasu et al., 1998).

3 SHELL DYNAMICS NUMERICAL ANALYSIS

3.1 Positional formulation

Considering the auxiliary reference, ξ_1, ξ_2, ξ_3, a shell element from its initial, B_0, and current, B_1, of the finite element, can be mapped by the functions, f's, as may see in figure 2.

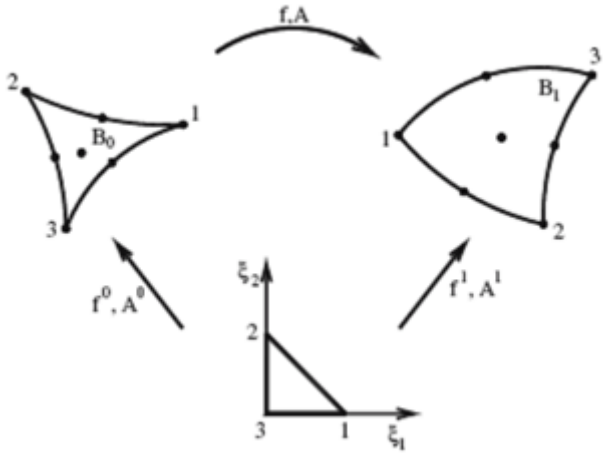

Figure 2: Positional Mapping (Coda and Paccola, 2007)

Shell structures are solids with one dimension much larger than the others. Therefore, the mid surface of the element serves as a reference to the solid mapping. The mappings f^0 and f^1,

from an auxiliary nondimensional space respectively to the initial and current configurations are given by:

$$f_i^0 = X_i = N_j(\xi_1, \xi_2, \xi_3)X_{ij} + \frac{h_0}{2}\xi_3 N_j(\xi_1, \xi_2)e_{ij}^0, \tag{11}$$

$$f_i^1 = x_i = N_j(\xi_1, \xi_2, \xi_3)x_{ij} + \frac{h_0}{2}\left[\xi_3 + N_j(\xi_1, \xi_2)a_j\xi_3^2\right] N_j(\xi_1, \xi_2)\bar{G}_{ij}, \tag{12}$$

where X_i are the coordinates on configuration B_0, x_i the coordinates on B_1, $\bar{G}_{ij}$ are the nodal values (unknowns) for the generalized vector at node j at final configuration, h_0 is the initial thickness, e_i^0 is the $i-th$ component of the unitary vector $\vec{e^0}$, normal to the middle surface at initial and a_j is the strain rate along thickness.

Thus, it is determined the mapping between the initial and final position:

$$\mathbf{f} = f(\mathbf{X}) = (\mathbf{f}^1) \circ (\mathbf{f}^0)^{-1}, \tag{13}$$

and the gradient A of mapping function may be expressed by:

$$\mathbf{A} = \nabla f = (\mathbf{A}^1)(\mathbf{A}^0)^{-1}. \tag{14}$$

After evaluating the gradient A, the Green strain tensor is given by:

$$E_{ij} = \frac{1}{2}[A_{ki}A_{kj} - \delta_{ij}] = \frac{1}{2}[C_{ij} - \delta_{ij}], \tag{15}$$

where C_{ij} is the right Cauchy-Green stretch tensor and δ_{ij} the Kroeneker delta. Thus, the adopted strain measure in the present work is the Green-Lagrange deformation.

The following quadratic strain energy per unit of initial volume is adopted (see Ogden (1984)):

$$u_e = \frac{1}{2}E_{ij}C_{ijkl}E_{kl}, \tag{16}$$

resulting into a linear elastic constitutive law relating second Piola– Kirchhoff stress and Green strain, usually known as Saint–Venant–Kirchhoff elastic law, i.e.:

$$S_{ij} = \frac{\partial u_e}{\partial E_{ij}} = C_{ijkl}Ekl \tag{17}$$

where C_{ijkl} are the components of the elastic constants tensor.

3.2 Time discretization

From preceding developments, it may be write the equilibrium equation as the minimization of the energy functional as:

$$\frac{\partial \mathbf{U}_e}{\partial x} - \mathbf{F} + \mathbf{M}\,\ddot{x} + \mathbf{C}\,\dot{x} = 0, \tag{18}$$

where **F** the external forces vector, **C** the dissipative matrix and **M** the mass matrix, constant in the formulation developed.

From the Newmark β method, the equilibrium equation, Eq. (18), for given instant $s+1$ becomes:

$$\left.\frac{\partial \mathbf{U}_e}{\partial x}\right|_{s+1} - \mathbf{F}_{s+1} + \frac{\mathbf{M}}{\beta \Delta t^2}\mathbf{x}_{s+1} - \mathbf{M}\,\mathbf{Q}_s + \mathbf{C}\mathbf{R}_s + \frac{\gamma \mathbf{C}}{\beta \Delta t} x_{s+1} - \gamma \Delta t \mathbf{C}\,\mathbf{Q}_s = 0 \tag{19}$$

where $\mathbf{Q}_s = \frac{x_s}{\beta \Delta t^2} + \frac{\dot{x}_s}{\beta \Delta t} + \left(\frac{1}{2\beta} - 1\right)\ddot{x}_s$ and $\mathbf{R}_s = \dot{x}_s + \Delta t(1-\gamma)\ddot{x}_s$.

Equation (19) represents a non-linear system, solved by the Newton-Raphson method.

4 PARTITIONED FLUID-STRUCTURE COUPLING

In this paper we study Neumann-Direchlet type explicit (weak) one-way and two-way coupling schemes for short duration problems, and the stability and conservative properties of structure and fluid dynamics solvers separately are well known (see e.g. Sanches and Coda (2013); Zienkiewicz and Taylor (2000) and Nithiarasu et al. (1998)), but energy and momentum conservation as well as a deep study on convergence properties of the coupling are going to be considered in a future work.

4.1 Forces and velocities transfers

As fluid and shell meshes are different and generated in an independent process, during the pre-processing step, for each fluid node i, a closest point Ps_i at shell mesh domain (Ω_s) is identified and stored (see Fig. 3). Subsequently, the fluid mesh is adapted moving the node i to the exact position of Ps_i.

For each shell node k , a closest point Pf_k on the fluid boundary related to the structure (Γ_s) is identified and stored.

The Dirichlet boundary conditions for node i are obtained from the shell point Ps_i. For viscous flow $\mathbf{u}_f(i) = \mathbf{u}_s(Ps_i)$ while for inviscid flow we adopt:

$$\mathbf{u}_f(i) = \mathbf{u}_f(i) + [(\mathbf{u}_s(Ps_i) - \mathbf{u}_f(i)) \cdot \mathbf{n}]\mathbf{n}. \tag{20}$$

where $\mathbf{u}_f$ is the fluid velocity vector, $\mathbf{u}_s$ is the shell velocity vector and **n**, the unity vector normal to Γ_s.

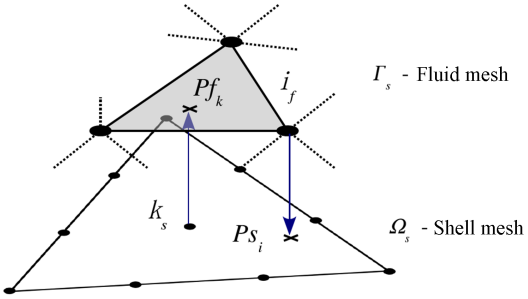

Figure 3: Transfer points

The Neumman boundary conditions for node k are obtained from fluid point Pf_k by the following expression:

$$q_{kj} = [\tau_{jl} n_l - p n_l]_{Pf_k}\,, \tag{21}$$

where the indexes *j* and l represent Cartesian direction and n_l is the l component form the normal vector to Γ_s.

4.2 Fluid mesh dynamic moving

A good mesh moving algorithm for fluid-structure interaction problems will adapt the fluid mesh to the solid movement with minimal of mesh distortion.

The Laplace equation would be a good choice for a mesh moving model (Kanchi and Masud, 2007), however it makes necessary to solve a new equation system. Therefore we adopted the same technique employed by Sanches and Coda (2014), which is based in the one employed by Teixeira (2001) . This technique consists on distribute the space mesh velocities and positions based on the distance to the boundary according to:

$$X_{f_i}^k = \frac{\sum_{j=1}^{ne} a_{kj} X_{s_i}^j}{\sum_{j=1}^{ne} a_{kj} + \sum_{l=1}^{nf} b_{kl}}, \tag{22}$$

where *ne* is the shell nodes number, *nf* is the fixed boundary (Γ_f) nodes number, a_{kj} is the weight coefficient that considers the shell movement influence, and b_{kl} is the coefficient that takes in account the fixed boundary influence and X_f and X_s may be respectively fluid mesh and shell velocities or fluid mesh and shell displacements.

The coefficients a and b are given by:

$$a_{kj} = \frac{1}{d_{kj}^{e1}} \tag{23}$$

and

$$b_{kl} = \frac{1}{d_{kl}^{e2}}, \tag{24}$$

where d_{kj} is the distance between the node *k* and the node *j* located at the moving boundary, d_{kl} is the distance between the node *k* and the node l located at fixed fixed boundary, and *e1*

and *e2* are numbers chosen by the operator which enable to adjust the boundary influence over the mesh movement. A good choice for open flow problems is $e1 = e2 = 4$, however for closed flows with large displacements a smaller number may present better results. It is important to notice that the mesh moving technique accounts only to structure's movement scale smaller than the dimensions of the fluid field.

4.3 Basic two-way coupling dynamic process

As the shell solver is implicit and the fluid solver explicit, a coupling scheme which enable sub-cycles of time steps is desirable. It is usual that time steps used for shell analysis are larger than the ones adopted for fluid modeling, therefore we suggest the scheme depicted on Fig. 4.

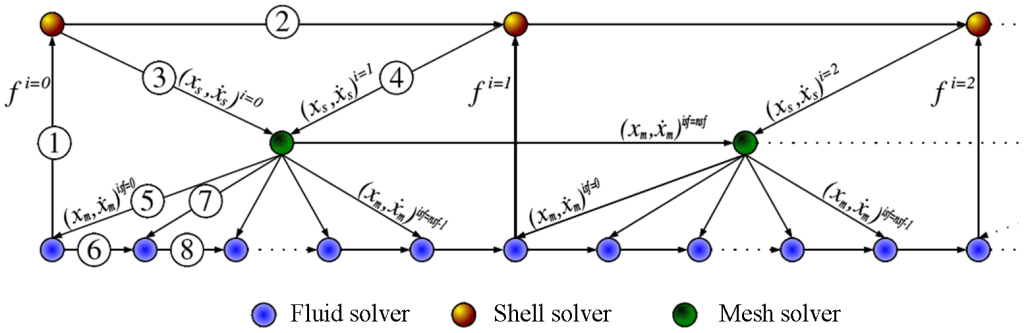

Figure 4: Coupling scheme adapted from Sanches and Coda (2013)

This scheme may be summarized as:

- At a given instant $t_s = i$, the structure is solved with the loads imposed by the flow (step 1), with a time step Δt_s, so that the velocities and positions at instant $t_s = i + 1$ are obtained (step 2).
- Shell positions variations inside the time interval Δt_s are approximated by a cubic polynomial, which is obtained based on $x_s(i)$, $\dot{x}_s(i)$, $x_s(i+1)$ and $\dot{x}_s(i+1)$ (steps 3 and 4). From this polynomial we can find the shell velocities and positions for each fluid time step $\Delta t_f = (\Delta t_s)/nsf$. Following, the fluid mesh movement is obtained from equations (22), (23) and (24) (steps 5 and 7).
- Fluid Dirichlet boundary conditions are obtained from the shell movement and the fluid is solved using time steps Δt_f (steps 6 and 8) until reach the instant $t_f = i * nsf$, when fluid loads are imposed to the structure and the process restart.

For one-way coupling, we just skip all the arrows from shell solver to mesh solver and from mesh solver to fluid solver in figure 4.

5 NUMERICAL STUDIES

We have chosen a simulation made by the laboratory from Institut Universitaire des Systèmes Thermiques Industriels (IUSTI) Giordano et al. (2005) to validate and verify the effectiveness of the present algorithm, as the author provides experimental and numerical results for this case.

Following, we use a three-dimensional example to ensure the effectiveness and robustness of the algorithm in more complex examples.

5.1 Shock wave on deforming panel

This problem is a experiment made by IUSTI's Laboratory. The test consists of a deforming panel fixed on a base, assumed infinitely rigid, inside a shock tube (T80) where a shock propagates hitting the panel. One pressure sensor is located on the top of the tube displaced 10mm to the left of the panel. Moreover, the horizontal displacement of the top of the panel is also measured. The experiment set up is shown in Fig. 5.

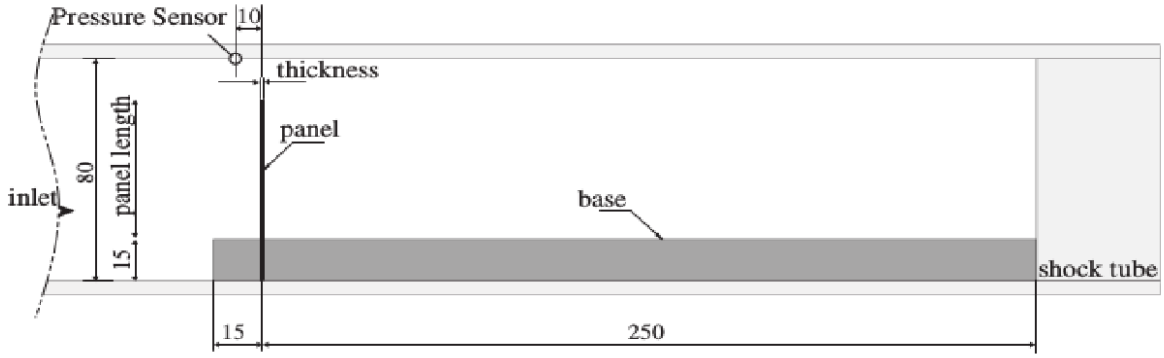

Figure 5: Shock tube experiment (Giordano, 2005).

The shock wave enters the tube from the left side at Mach 1.21. The fluid, air, is initially at rest, with pressure 10^5 kPa and temperature 293 K. The panel is 40 mm width and 1 mm thick, with Young's modulus of 220 GPa and specific mass of 7600 kg.m^{-3}. The experiment is fully described by Giordano et al. (2005).

The problem is discretized by 56982 tetrahedral linear elements and 16993 nodes for the fluid domain and by 40 triangular isoparametric cubic elements and 244 nodes for the shell. The meshes are presented in Fig. 6

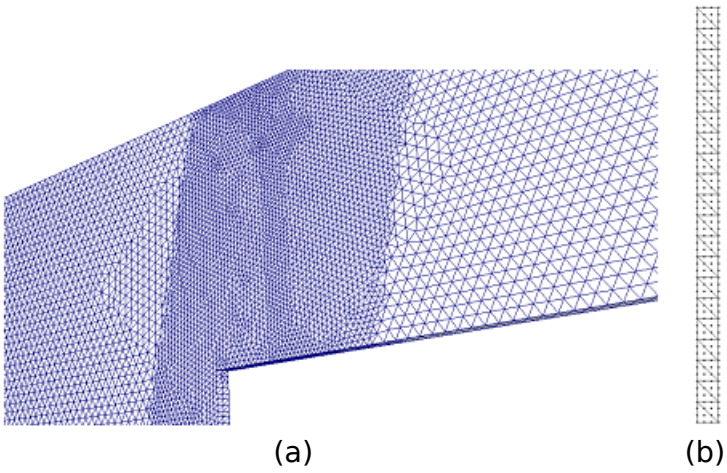

Figure 6: Meshes (a) fluid and (b) solid. (Sanches, 2011).

Firstly we simulate the problem using the two-way coupling scheme with time step dt equal to the fluid and the structure of 5.10^{-7} s. The obtained results are very similar to the experimental data and also agree with reference numerical results, as one can see from Fig. 7.

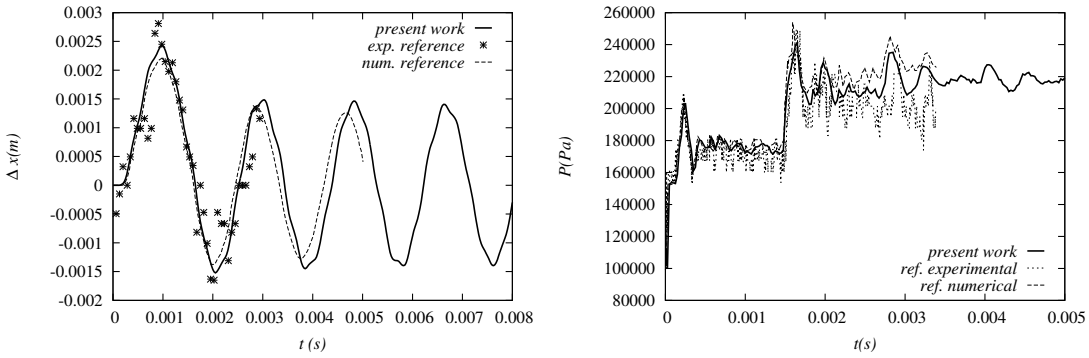

(a) horizontal displacements (b) Pressure at sensor position

Figure 7: Two-way coupling results with 1 time subcycle compared to Giordano (2005).

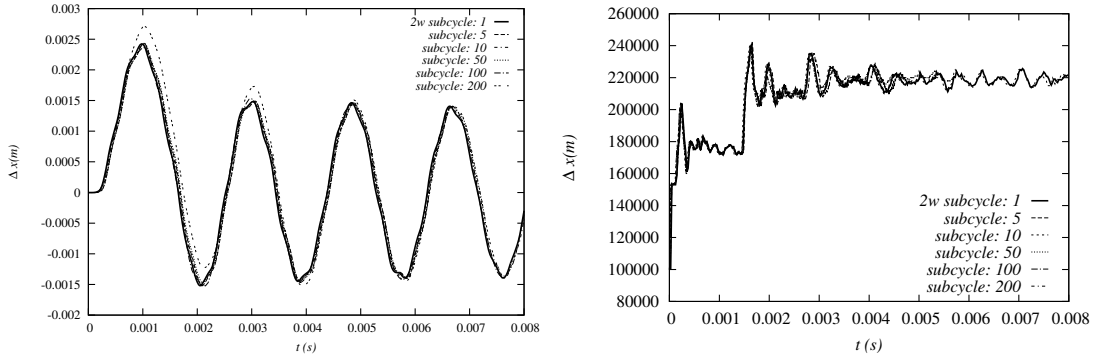

(a) horizontal displacement (b) pressure at sensor position

Figure 8: Two-way coupling with time subcycles

Following we study the two-way coupling scheme behavior with time subcycles between fluid and structure. Firstly we keep the fluid time step fixed as 0.5 μs and change the structure time step by using 5, 10 and 100 subcycles (time steps for the structure (shell dt = 2.5x10^{-6} s, 5x10^{-6} s and 5x10^{-7} s, respectively) between fluid and structure, and secondly we change the fluid time step to 1 μs and 0,00625 μs for 50 and 200 subcycles, respectively. It is noted that, in Fig. 8, employing 50 subcycles the responses remain almost the same, and at 200 subcycles the answer is still very close to the two-way reference (1 subcycle).

After checking the two-way model performance, we verify if the computational effort can be reduced by using the one-way coupling scheme. Thus, the previous analysis is repeated considering now the one-way coupling scheme. The results are shown in Fig. 9 and it can be noticed the difference from the 1 subcycle to the others is greater than the same for the two-way scheme.

In Figure 10, we compare the two-way coupling results with 1 subcycle to one-way results with 1 and 200 subcycles (best and worst one-way coupling results). One can observe that even in the best one-way case there are differences from the two-way coupling, which points to be necessary a deep analysis before employing one-way tchniques.

The maximum relative difference in displacement from one-way to two-way coupling is 17.166% for 1 subcycle and 22.558% for 200 subcycles. This shows that even for problems like

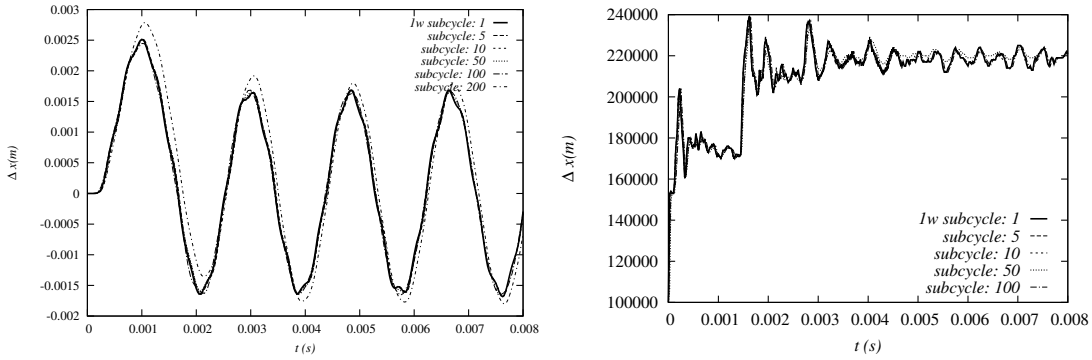

(a) horizontal displacement (b) pressure at sensor position

Figure 9: One-way coupling with time subcycles

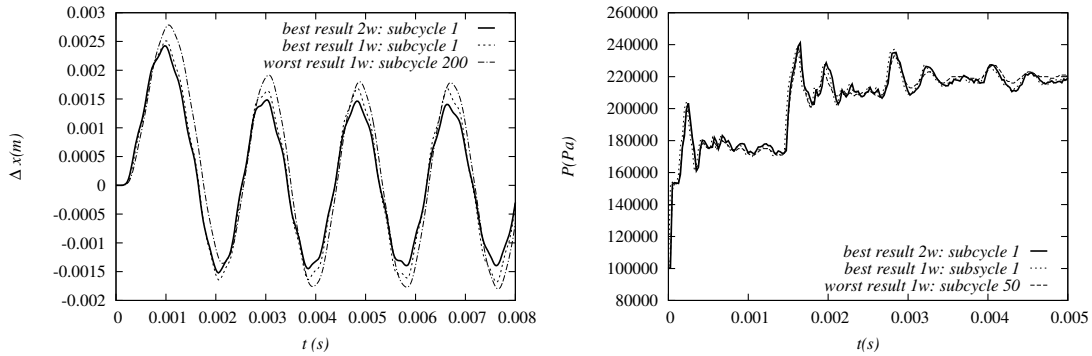

(a) horizontal displacement (b) pressure at sensor position

Figure 10: Best and worst one-way results compared with the best two-way.

this, with small amplitude, mistakes can be significant when employing the one-way scheme. Regarding pressure we notice a maximum relative difference of 0.890% at 1 subcycle and 2.470% at 50 subcycles. This shows that one-way coupling can be used satisfactorily to analyze pressure, reducing therefore computational efforts.

Looking for conditions where one-way coupling can be employed more precisely, saving lower computational costs and better data accuracy, we increase the thickness of the panel, making the displacement small enough to not disturb significantly the fluid flow.

Thickness 2.5 mm Changing the panel thickness from 1 mm to 2.5 mm panel thickness, the results are much more close to the two-way case as presented in Fig. 11. In this case, the maximum relative difference of 8.570% at 1 subcycle and 7.011% at 50 subcycles. Analyzing pressure, maximum relative difference of 0.422% for 1 subcycle and 2.336% for 50 subcycles.

5.2 3D explosion of a flat panel

As previous section ensured the effectiveness of the algorithm for two-dimensional examples, this section applies this procedure to one more complex three-dimensional model. In this example one initially flat panel is submitted to a explosion. The air is initially at rest, with pressure $p = 100$ kPa, and temperature $T = 290.36$ K. The explosion is modeled by a bulb of diameter $d = 1$ m with gas initially at rest, with pressure $p = 2967$ kPa and temperature

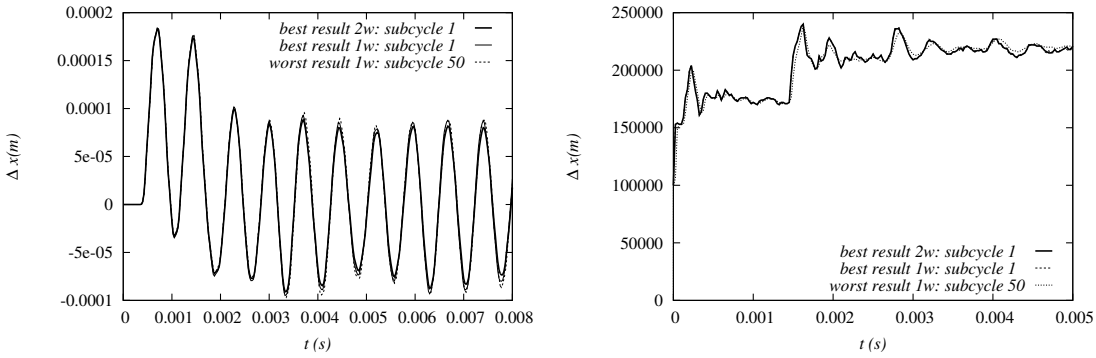

(a) displacements (b) pressure at sensor position

Figure 11: Results for the 2.5 mm thick panel

$T = 1134.85$ K. The panel is 4 m height, 8 m widht and 10 cm thick, made of a material with Young's modulus of 25 GPa and density of 2300 kg.m^{-3}, simulating a concrete wall.

As the problem may be considered symmetric, we discretize only half of it and apply symmetry conditions over the plane xy as one can see from Fig. 12. The fluid domain is discretized by 281595 tetrahedral linear elements and 49491 nodes and the solid domain has 72 triangular cubic shell elements and 361 nodes.

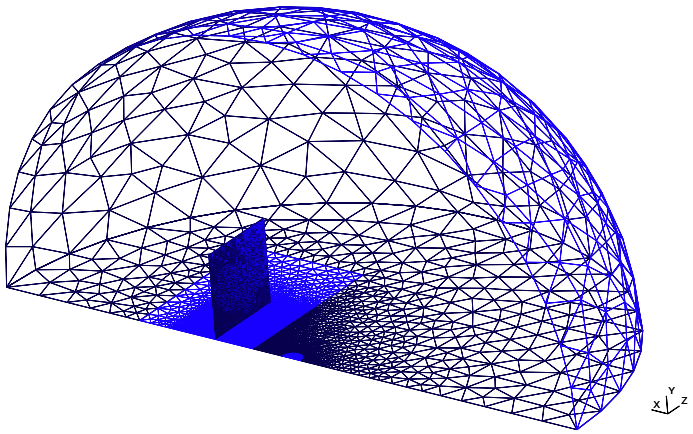

Figure 12: Fluid and solid mesh

The panel is fully clamped in the base. The fluid presents frictionless conditions wall (null normal speed) in the base, normal component of speed equals to the structure normal component of velocity at the interface fluid/structure and the boundary conditions on the spherical surface are extrapolated from the area to prevent wave reflection. The time step of the structure is $\Delta t_s = 10^{-7}$ s and we used 10 subcycles for the fluid dynamics.

Pressure distribution for instants t=1 ms and t= 7.5 ms are depicted in fig. 13.

6 CONCLUSION

In this paper we studied the performance of a partitioned scheme for compressible flow-shell structure coupling, in the context of short duration events, such as blast waves.

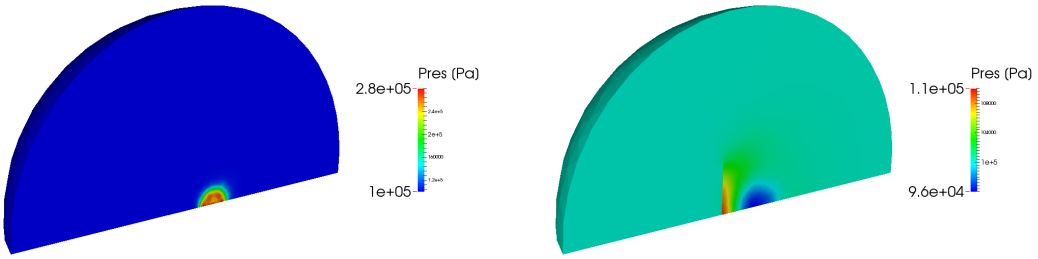

(a) 1 ms (b) 7.5 ms

Figure 13: Pressure analysis

Separately both, fluid dynamics algorithm, explicit and with time integration based on characteristics, and the nonlinear shell dynamics solver, implicit and based on positions, showed to be efficient and robust.

The main question to answer is if for short durations problems it is worth to employ two-way partitioned algorithm. From our analysis, we conclude that in some cases (with not so small displacements) the results showed that the one-way algorithm produces results considerably wrong, even for the initial cycles.

Another option to reduce computational cost is to use the two-way coupling with subcycles of time between fluid and structure, reducing the computational effort and, according to the numerical tests, producing good results.

ACKNOWLEDGEMENTS

The first author thank God for the gift of life and knowledge, for giving such opportunity through this present work. He also thanks the advisor Rodolfo A. K. Sanches, for believing him and be an example of a professional. To his parents, who share the same joy that his son throughout the academic journey. CNPq for grant Scientific Initiation scholarship, through which the production of this study was possible. The SET department, for giving space and computing resources and infrastructure, and all the people who, in some way, contributed to this work. The body of teachers at the EESC-USP, offering and motivate their students to crave academic opportunities. The CILAMCE 2015 committee, for affords this opportunity.

REFERENCES

Bethe H.A., Fuchs K., Hirschfelder J.O., Magee J.L., Peierls R.E., and von Neumann J. Blast wave. research report, Los Alamos Scientific Laboratory of the University California, Los Alamos, New Mexico, USA, 1947.

Bonet J., Wood R.D., Mahaney J., and Heywood P. Finite element analysis of air supported membrane structures. *Computer Methods in Applied Mechanics and Engineering*, 190(5-7):579 – 595, 2000. ISSN 0045-7825. doi:DOI: 10.1016/S0045-7825(99)00428-4.

Coda H. Análise não linear geométrica de sólidos e estruturas: uma formulação posicional baseada no mef. *Texto complementar para concurso de professor titular. São Carlos: Escola de Engenharia de São Carlos*, 2003.

Donea J., Giuliani S., and Halleux J.P. An arbitrary lagrangian-eulerian finite element method for transient dynamic fluid-structure interactions. *Computer Methods in Applied Mechanics and Engineering*, 33(1-3):689 – 723, 1982. ISSN 0045-7825.

Giordano J., Jourdan G., Burtschell Y., Medale M., Zeitoun D.E., and Houas L. Shock wave impacts on deforming panel, an application of fluid-structure interaction. *Shock Waves*, 14:103–110, 2005. ISSN 0938-1287.

Kanchi H. and Masud A. A 3d adaptive mesh moving scheme. *International Journal for Numerical Methods in Fluids*, 54(6-8):923–944, 2007. ISSN 1097-0363. doi:10.1002/fld.1512.

Nithiarasu P., Zienkiewicz O.C., Sai B.V.K.S., Morgan K., Codina R., and Vazquez M. Shock capturing viscosities for the general fluid mechanics algorithm. *International Journal for Numerical Methods in Engineering*, 28(9):1325–1353, 1998. ISSN 0271-2091.

Ogden R. Non-linear elastic deformations. *Engineering Analysis*, 1(2):119 – 119, 1984. ISSN 0264-682X.

Prümmer R. History of shock waves, explosions and impact – a chronological and biographical reference, peter o. k. krehl. *Propellants, Explosives, Pyrotechnics*, 34(5):458–458, 2009. ISSN 1521-4087. doi:10.1002/prep.200990012.

Sanches R.A. and Coda H.B. Unconstrained vector nonlinear dynamic shell formulation applied to fluid structure interaction. *Computer Methods in Applied Mechanics and Engineering*, 259(0):177 – 196, 2013. ISSN 0045-7825. doi:http://dx.doi.org/10.1016/j.cma.2013.02.016.

Sanches R.A.K. *Sobre o acoplamento fluido-casca utilizando o método dos elementos finitos*. D.Sc. Thesis, Universidade de São Paulo, 2011.

Sanches R.A.K. and Coda H.B. On fluid-shell coupling using an arbitrary lagrangian-eulerian fluid solver coupled to a positional lagrangian shell solver. *Applied Mathematical Modelling*, 38(14):3401 – 3418, 2014. ISSN 0307-904X. doi: http://dx.doi.org/10.1016/j.apm.2013.11.025.

Taylor C.A., Hughes T.J.R., and Zarins C.K. Finite element modeling of blood flow in arteries. *Computer Methods in Applied Mechanics and Engineering*, 158(1-2):155 – 196, 1998. ISSN 0045-7825. doi:10.1016/S0045-7825(98)80008-X.

Teixeira P.R.F. *Simulação Numérica da interação de escoamentos tridimensionais de fluidos compressíveis e incompressíveis e estruturas deformáveis usando o método de elementos finitos*. Doutorado em engenharia civil, Escola de Engenharia, Universidade Federal do Rio Grande do Sul, Porto Alegre, 2001.

Zienkiewicz O.C. and Roriva R.C. *Search for a general fluid mechanics algorithm*. Centro Internacional de Métodos Numéricos en Ingeniería, 1993.

Zienkiewicz O.C. and Taylor R.L. *The Finite Element Method, v3: Fluid Dynamics*. Butterworth-heinemann Linacre house, 2000.